Available online at www.sciencedirect.com

ScienceDirect

IFAC Papers Online CONFERENCE PAPER ARCHIVE

IFAC PapersOnLine 50-1 (2017) 14533–14538

Path planning with fractional potential fields for autonomous vehicles

Julien Moreau [*,***] **Pierre Melchior** [*] **Stéphane Victor** [*]
François Aioun [**] **Franck Guillemard** [**]

[*] *IMS – UMR 5218 CNRS, Université de Bordeaux/Bordeaux INP*
351 cours de la Libération, 33405 Talence cedex – France
Email: firstname.lastname@ims-bordeaux.fr
[**] *PSA Groupe*
Chemin de Gisy, 78140 Vélizy-Villacoublay cedex – France
Email: francois.aioun@mpsa.com
[***] *OpenLab PSA Groupe-IMS Bordeaux*

Abstract: Path planning is an essential stage for mobile robot control. It is more newsworthy than ever in the automotive context and especially for autonomous vehicle. Also, path planning methods need to be adaptive regarding life situations, traffic and obstacle crossing. In this paper, potential field methods are proposed to cope with these constraints and autonomous vehicles are considered equipped with all necessary sensors for obstacle detection. In this way, Ge&Cui's attractive potential field and fractional attractive potential field have been adapted to the context of autonomous vehicles. In this way, this latter method ensures better stability degree robustness with controlled vehicle acceleration.

© 2017, IFAC (International Federation of Automatic Control) Hosting by Elsevier Ltd. All rights reserved.

Keywords: Path planning, automotive, autonomous vehicle, potential field, fractional potential field

1. INTRODUCTION

Autonomous driving is going to be the heart of public transports in the future. Autonomous vehicles have the potential to improve passenger's safety, reduce travel time and improve the comfort of the passengers. As a consequence car manufacturers invest in the conception and the equipment of their vehicles with advance systems for assistance. In urban areas, intersections are considered as bottlenecking; more than 44 % of all the accidents reported in the United States arise in intersection zones and are responsible for 8,500 deaths and approximately 1 million wounds every year. Besides, the traffic delays generated by intersections lead to enormous losses of resources. Therefore, autonomous vehicles answer to these issues.

The urban area represents the sensitive case for autonomous vehicles. Indeed, this kind of environment is variable: autonomous vehicles need to be adaptive regarding life situations, traffic and obstacle crossing. In this paper, autonomous vehicles are considered equipped with all necessary sensors for obstacles detection.

These recent years, path planning for autonomous vehicles has been widely studied in literature. In Makarem and Gillet (2011), a navigation function for autonomous vehicles has been developed but no pedestrians have been considered in this method. Another interesting method called "tentacles method" has been developed in A. Chebly and Charara (2015). The idea is to deploy a set of virtual tentacles with different curves in front of the autonomous vehicle, each tentacle representing a possible vehicle path. Each path is then evaluated according to a set of criteria. The main advantage is that the vehicle is able to navigate with no "a priori" on the environment. However, this method could lead to behaviors unreadable by the driver.

Potentials field methods are common path planning methods in mobile robotics (Inarn et al. (2012)). These methods have been already used for Unmanned Aircraft System (UAV) in Zhan et al. (2014), Andrew-Fields (2014) and Liu et al. (2016). Moreover, they have also been used in automotive especially for collision avoidance in Shibata et al. (2014) however no extension for a complete navigation has been developed.

In order to use potential field for autonomous vehicle navigation, a strategic schematic has been developed (see Fig. 1). This schematic has three stages:
- the strategic stage: data is collected and processed from perception sensors in order to create an immediate virtual map of the autonomous vehicle with obstacle informations (velocity, position, ...) and targets;
- the tactical stage: from the previous informations, a force resulting of an attractive and repulsive potential field combination is generated and according to a simple model (punctual mass model), the ideal position, velocity and acceleration are generated by simulating the motion of a charged particle subjected to this generated force;
- the operational stage: the ideal position, velocity and acceleration from the previous stage are used as references as a classic control loop, the controller using the deviation between references and measures in order to generate a steering angle of wheel β_w and a wheel torque T_w.

In this paper, only the tactical stage is presented. Indeed, the strategic stage is a data processing problem whereas

2405-8963 © 2017, IFAC (International Federation of Automatic Control) Hosting by Elsevier Ltd. All rights reserved.
Peer review under responsibility of International Federation of Automatic Control.
10.1016/j.ifacol.2017.08.2076

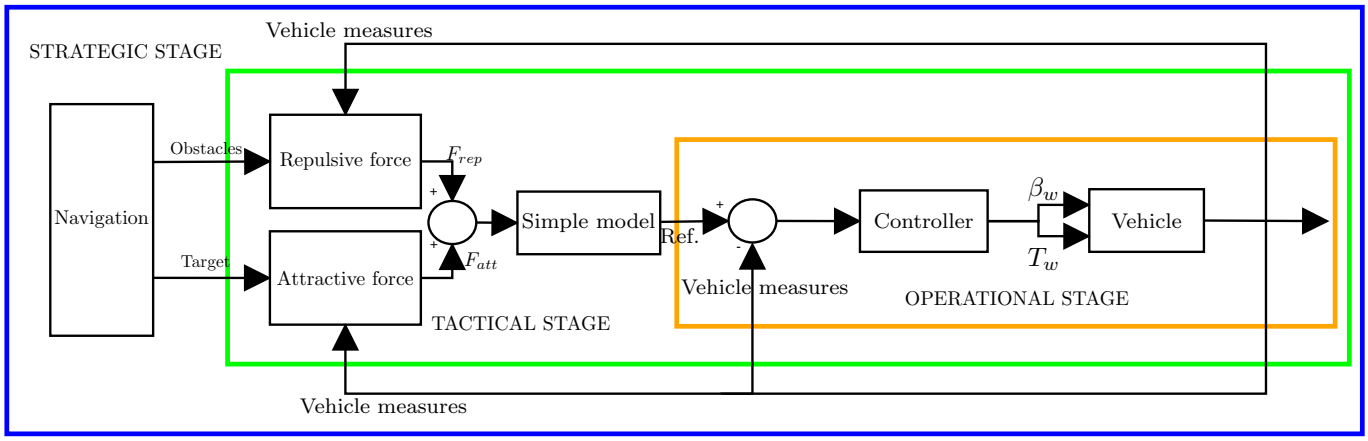

Fig. 1. Plan of regulation at three levels: strategic (blue), tactical (green) and operational (orange))

the operational is a control problem. The fractional differentiation has been already used in automotive (Morand et al. (2016)). This present work is based on the extension of the work developed in Melchior et al. (2001),Melchior et al. (2003) and Metoui et al. (2009) on fractional potential field. Firstly, the fractional potential field method is presented in section 2. After that, section 3 shows extensions on fractional potential field method to autonomous vehicle. A set of simulation results is presented in section 4, to finally conclude in section 5.

2. FRACTIONAL POTENTIAL FIELD

In motion control, a charged particle is subject to:
-an attractive potential field tied to the target
-and a repulsive one tied to obstacles for avoidance.
Compared to a classic potential field, a fractional definition of the potential field allows to create a less constrained potential field curve.

2.1 Fractional repulsive potential field

Let us consider the fractional repulsive potential field U (see Fig. 2) defined by :

$$U(r) = \frac{r^{n-2} - r_{max}^{n-2}}{r_{min}^{n-2} - r_{max}^{n-2}} \; for \; r_{min} < r \leq r_{max},$$

where r is the distance of the particle to the considered obstacle, r_{min} and r_{max} the boundaries of the repulsive potential field and n the fractional order.

The potential field can be shaped by using the parameter n (see Fig. 3). For example, when a charged particle is on a direct course to an obstacle, the higher the parameter n, the farther from the obstacle the move of the particle. Thus, the parameter n can be interpreted as a danger parameter.

The potential field is applied to each obstacle and free road is obtained by the truncation of the potential map (Melchior et al. (2003)). The resulting force applied to the particle is given by:

$$\overrightarrow{F} = -grad(\overrightarrow{U}).$$

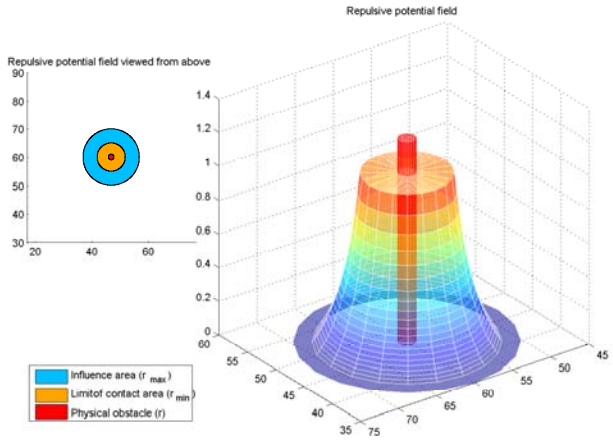

Fig. 2. Fractional repulsive potential field created around an obstacle

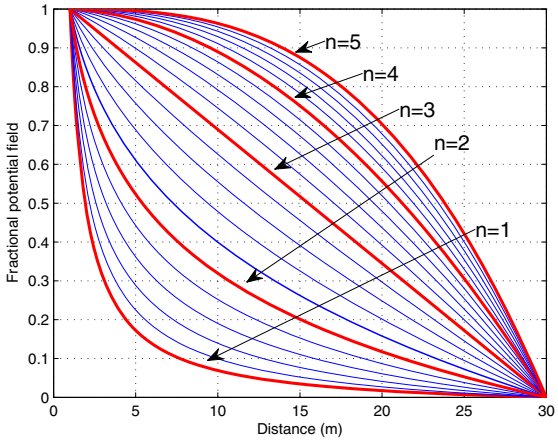

Fig. 3. Influence of parameter n on the potential field

2.2 Fractional attractive potential field

The resulting force expressed by Ge and Cui (2002) is given by:

$$\overrightarrow{F} = \alpha_p(\overrightarrow{x}_{target} - \overrightarrow{x}) + \alpha_v(\overrightarrow{v}_{target} - \overrightarrow{v}) \qquad (1)$$

where α_p and α_v are weighting coefficients, the particle position $\overrightarrow{x}$ and the target position $\overrightarrow{x}_{target}$, the particle velocity $\overrightarrow{v}$ and the target velocity $\overrightarrow{v}_{target}$.

For the fractional attractive potential field, an extension of equation (1) gives:

$$\overrightarrow{F} = \alpha_p(\overrightarrow{x}_{target} - \overrightarrow{x}) + \alpha_v \frac{d^n}{dt^n}(\overrightarrow{v}_{target} - \overrightarrow{v}), \qquad (2)$$

where the fractional derivative of the position is considered instead of the velocity.

Let us consider a punctual mass model:

$$G(s) = \frac{X(s)}{F(s)} = \frac{1}{Ms^2} \qquad (3)$$

where s is the Laplace variable, *X(s)* the Laplace transform of the vehicle position and *F(s)* the Laplace transform of the resulting force (repulsive or attractive).

According to equations (2) and (3), the fractional attractive potential field can be interpreted as a position controller. This interpretation leads to the elementary control loop schematic (see Fig. 4).

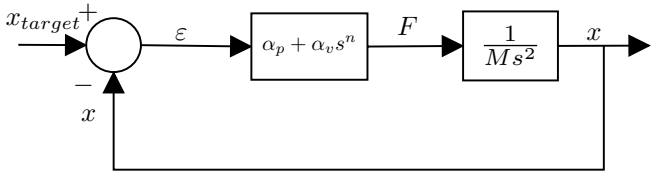

Fig. 4. Elementary control loop schematic with Ge&Cui's attractive potential field when $n = 1$ and fractional attractive potential field in other cases

The open-loop expression associated to this schematic is expressed as $\beta(j\omega) = \frac{\alpha_v(j\omega)^n + \alpha_p}{M(j\omega)^2} = \frac{1+(\frac{j\omega}{\omega_c})^n}{\frac{M}{\alpha_p}(j\omega)^2}$. In high frequencies, it then becomes:

$$\beta(j\omega) \approx \frac{\alpha_v}{M(j\omega)^{2-n}}, for\ \omega >> \omega_c = \frac{\alpha_p}{\alpha v}^{\frac{1}{n}} \qquad (4)$$

or else,

$$\beta(j\omega) \approx \left(\frac{\omega_{ug}}{j\omega}\right)^{n'} \qquad (5)$$

where $n' = 2 - n$ and the unit gain frequency:

$$\omega_{ug} = \left(\frac{\alpha_v}{M}\right)^{\frac{1}{n'}}. \qquad (6)$$

Such an open-loop is expressed by a fractional order n' and the damping ratio is then given by (Oustaloup et al. (2014)):

$$\xi = -cos(\frac{\pi}{n'}). \qquad (7)$$

In this case, the damping ratio only depends on the parameter n' and it is independent of the model parameters. In this way, robustness of stability degree relative to the vehicle mass variation is ensured.

3. APPLICATION TO THE AUTONOMOUS VEHICLE

In this section, the drawbacks of classic attractive potential field when applied to the autonomous vehicle are presented. A solution using the concept of way-point is proposed. Finally, an upgrade of this solution using the fractional attractive potential field is explained.

3.1 Limits of classic Ge&Cui's attractive potential field in autonomous vehicle context

According to Fig. 4, the Laplace transform of the vehicle acceleration can be expressed (with $n = 1$) according to:

$$\Gamma(s) = \frac{\frac{\alpha_v}{\alpha_p}s^3 + s^2}{\frac{M}{\alpha_p}s^2 + \frac{\alpha_v}{\alpha_p}s + 1} X_{target}(s). \qquad (8)$$

Consequently, two main problems may occur with this definition. First, this transfer function is not proper (numerator degree higher than denominator one) leading to implementation problems. The second problem concerns the target position: the farther the target, the greater the attractive force magnitude and the greater the vehicle acceleration magnitude. Thus, if the vehicle acceleration is too high, it could be uncomfortable for passengers and in a worst case, the system limits may be reached.

3.2 Classic attractive potential field with limitation of vehicle acceleration

First of all, the causality problem can be fixed by using the vehicle velocity. In this way, vehicle velocity is used instead of the derivative of the vehicle position. However, the target velocity needs to be added as an input signal as illustrated on Fig. 5.

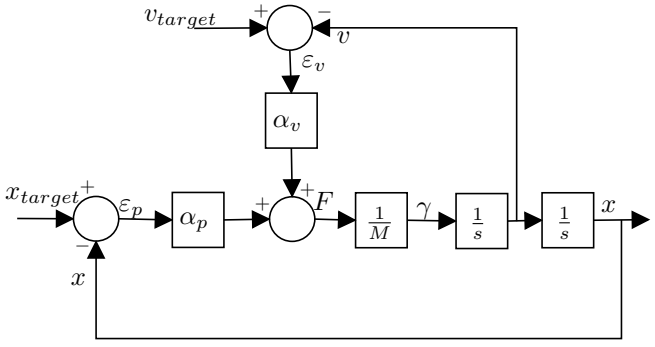

Fig. 5. Control loop schematic using attractive potential field and velocity

In this way, the vehicle acceleration becomes:

$$\Gamma(s) = \frac{\frac{\alpha_v}{\alpha_p}s^2}{\frac{M}{\alpha_p}s^2 + \frac{\alpha_v}{\alpha_p}s + 1} V_{target}(s) + \frac{s^2}{\frac{M}{\alpha_p}s^2 + \frac{\alpha_v}{\alpha_p}s + 1} X_{target}(s) \qquad (9)$$

In order to limit the acceleration to a γ_{max}, equation (9) becomes with $s = j\omega$:

$$\max|\Gamma(j\omega)| \leq \max\left|\frac{\frac{\alpha_v}{\alpha_p}(j\omega)^2}{\frac{M}{\alpha_p}(j\omega)^2+\frac{\alpha_v}{\alpha_p}(j\omega)+1}\right||V_{target}(j\omega)| + \max\left|\frac{(j\omega)^2}{\frac{M}{\alpha_p}(j\omega)^2+\frac{\alpha_v}{\alpha_p}(j\omega)+1}\right||X_{target}(j\omega)| \quad (10)$$

with a stationary target, $V_{target} = 0$ and thus, the attractive potential field coefficients can be expressed as:

$$\alpha_v = 2\xi\sqrt{\alpha_p M} \text{ and } \alpha_p \leq \frac{\gamma_{max} M}{|X_{target}|}. \quad (11)$$

These equations show that the target needs to be stationary and not too far from the vehicle in order to limit the acceleration. In the light of these constraints, a set of targets may be added throughout the vehicle path. These targets are called waypoints. The vehicle has to only consider the closest waypoint as attractive point, after reaching it, the following waypoint is used as the following attractive point, and until the end.

3.3 Fractional attractive potential field with limitation of vehicle acceleration

In the same way, a similar schematic can be established in the fractional case (see Fig 6).

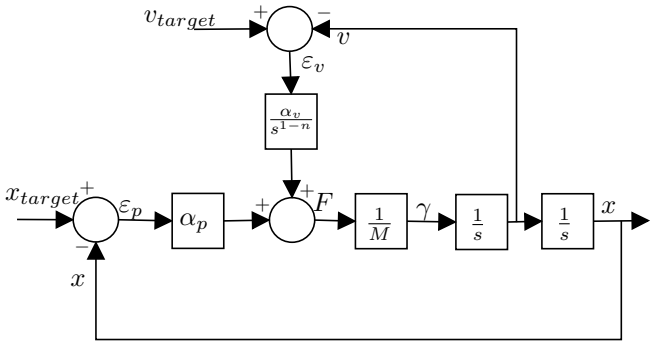

Fig. 6. Fractional attractive potential field with causality

In that case, the vehicle acceleration becomes:

$$\Gamma(s) = \frac{\frac{\alpha_v}{\alpha_p}s^{n+1}}{\frac{M}{\alpha_p}s^2+\frac{\alpha_v}{\alpha_p}s^n+1}V_{target}(s) + \frac{s^2}{\frac{M}{\alpha_p}s^2+\frac{\alpha_v}{\alpha_p}s^n+1}X_{target}(s). \quad (12)$$

In order to limit the acceleration to a γ_{max}, equation (12) then becomes:

$$\max|\Gamma(j\omega)\| \leq \max|\frac{\frac{\alpha_v}{\alpha_p}(j\omega)^{n+1}}{\frac{M}{\alpha_p}(j\omega)^2+\frac{\alpha_v}{\alpha_p}(j\omega)^n+1}||V_{target}(j\omega)| + \max|\frac{(j\omega)^2}{\frac{M}{\alpha_p}(j\omega)^2+\frac{\alpha_v}{\alpha_p}(j\omega)^n+1}||X_{target}(j\omega)|. \quad (13)$$

Considering a stationary target, $V_{target} = 0$ and equation (6), the expression of the attractive potential field coefficient is expressed as:

$$\alpha_v = M\omega_{ug}^{n'} \text{ and } \alpha_p \leq \frac{\gamma_{max} M}{|X_{target}|}. \quad (14)$$

4. SIMULATION

4.1 Acceleration constraint simulation

The autonomous vehicle is attracted by a single waypoint according to the attractive potential field theory. The attractive potential field coefficients are chosen in accordance with expressions (11) where $\xi = 1$ (without damping), $M = 750kg$ (light vehicle) and the waypoint is placed 100m farther than the vehicle. An acceleration limit is fixed to 0.5g where g is the gravity acceleration. The Bode diagram of the sensitivity function $\frac{\Gamma(s)}{X_{target}(s)}$ (blue curve) and the acceleration constraint (green curve) are plotted on Fig 7). As expected, this choice of coefficient respects the acceleration constraint in the useful frequency band.

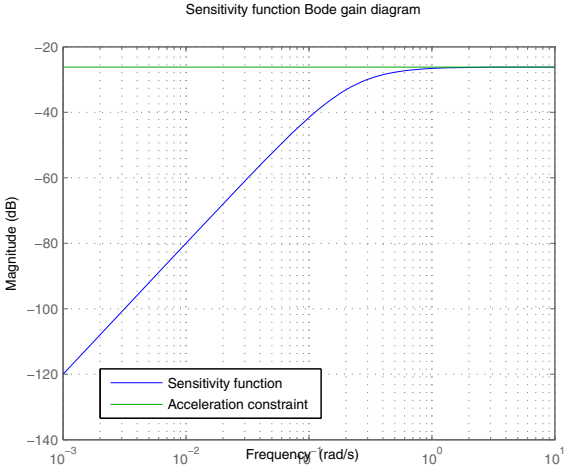

Fig. 7. Sensitivity function Bode gain diagram

To make sure that this constraint is well and truly respected, a simulation in a straight line is made. The attractive crossing point is placed in the point of coordinates (100m, 100m) while the vehicle is placed at the origin of the mark (0m, 0m). Figures 8, 9 and 10 represent respectively the position, the speed and the acceleration of the vehicle according to X-axis. The simulation being in a straight line and the crossing point being equidistant to the origin, only the temporal answers according to the X-axis are presented. Note that the vehicle reaches its destination in 30s with a maximum speed of 30km/h and maximum acceleration of 0.5g according to the acceleration constraint. If an obstacle appears during this motion, the trajectory will be locally adjusted in order to avoid it.

4.2 Stability degree robustness simulation

Now, the vehicle mass varies (single driver, full loaded vehicle,...). The classic and the fractional Ge&Cui's attractive potential field are designed for a maximum mass

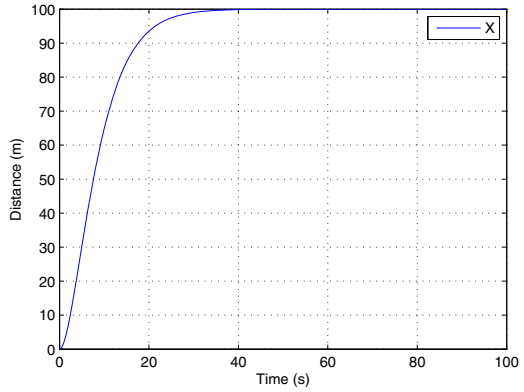

Fig. 8. Evolution of vehicle position

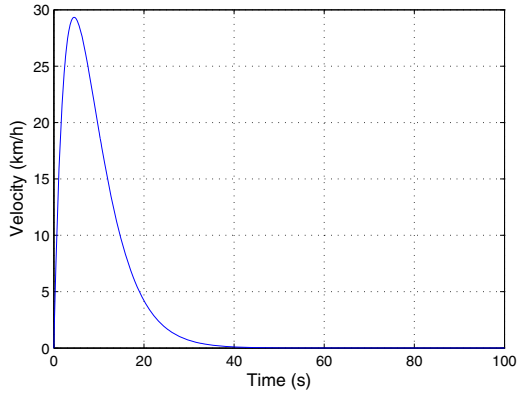

Fig. 9. Evolution of vehicle velocity

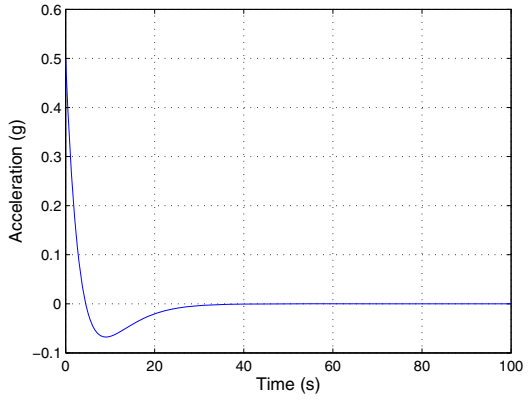

Fig. 10. Evolution of vehicle acceleration

and same unit gain frequency $\omega_{ug} = 0.39rad/s$. Then, the impact of mass variations on the stability degree is tested. Fig. 11 represents the Nichols chart of the open-loops for the classic cases (dotted line) and fractional ones (full line) for a maximum mass $M = 900\ kg$ (red), a medium mass $M = 750\ kg$ (green) and a minimum mass $M = 600\ kg$ (blue). In the classic case, mass variations lead to phase variations around the unit gain frequency ω_{ug} (the phase margin varies between 65 and 70 degrees) contrary to the fractional case where there is no phase variations around ω_{ug} (the phase margin is kept equal to 60 degree). Thus, in the fractional case, the phase margin is held, ensuring the stability degree.

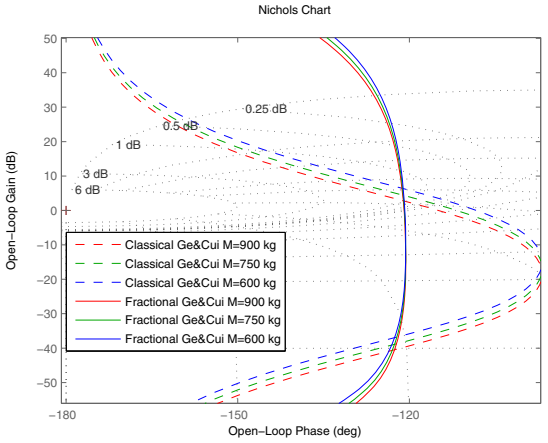

Fig. 11. Nichols chart of fractional and classic open-loops

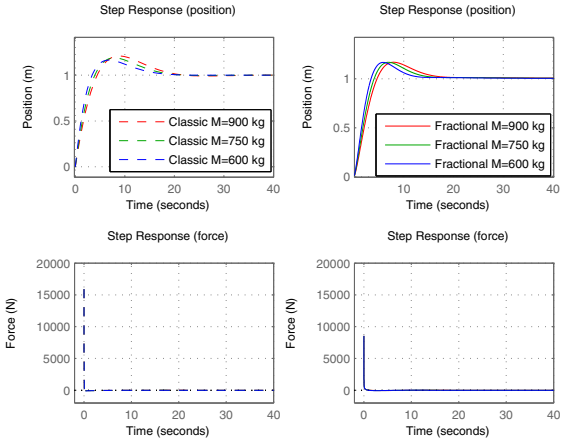

Fig. 12. Illustration of robustness with fractional potential field (right) compared to classic potential field (left)

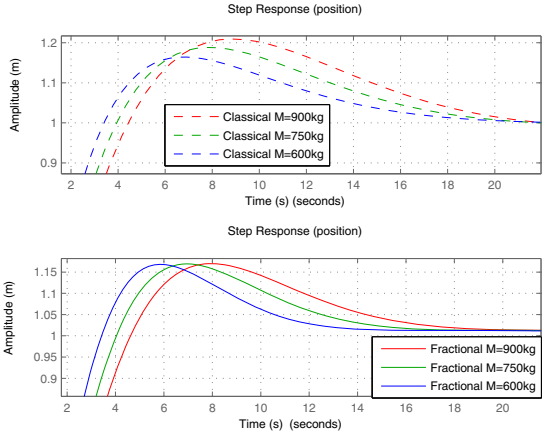

Fig. 13. Illustration of robustness with fractional potential field (down) compared to classic potential field (up)

Fig. 12 and Fig. 13 presents the step responses of the position for classic (dotted line) and fractional cases (full

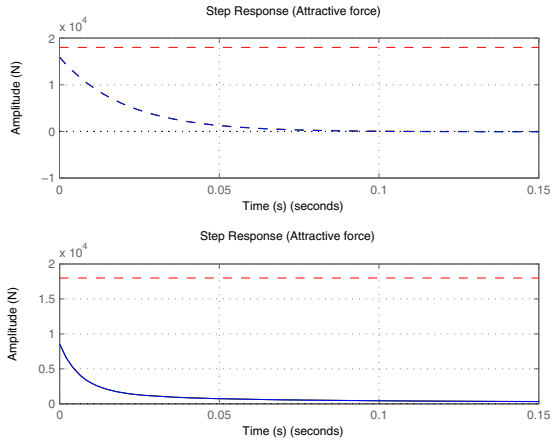

Fig. 14. Illustration of robustness with fractional potential field (down) compared to classic potential field (up) with corresponding attractive force (blue) and force constraint (red)

line) for a maximum mass (red), a medium mass (green) and a minimum mass (blue). In the fractional case, the damping is kept constant when the mass varies as opposed to the classic case. Finally, Fig. 14 is the corresponding attractive force (blue) with the force constraint (red). Both of them respects the force constraint however, in the fractional case, the curve is far below the limit as compared to the classic case. Thus, the fractional attractive potential field response time can be improved while it is not possible in the classic case.

5. CONCLUSION AND PERSPECTIVES

Research works on autonomous vehicle lead car manufacturers to focus on the urban area. This environment establishes a critical point for the autonomous vehicle because it is very variable due to the presence of numerous mobile obstacles (pedestrians) or due to the diversity of the road infrastructures (intersections, gyrating crossroads, ...). It is thus essential to develop adaptive path planning towards the environment of the autonomous vehicle.

In this way, a non exhaustive state of the art of these methods allows to put the potential field method in relation to the existing. The main advantage of this method is its adaptability which is a real need for autonomous vehicles. However, this method requires some modifications to become completely applicable to the autonomous vehicle.

From this perspective, an adaptation of the attractive potential has been proposed, enabling acceleration limits and stability degree robustness guarantee. A set of attractive points called waypoints are also introduced to better answer to the constraints of the autonomous vehicle.

The adaptation of the attractive potential field method is solved in this paper, the repulsive one needs to be scaled regarding the attractive potential field. Moreover, life situation scenarii need to be simulated and validated before testing this strategy on a real autonomous vehicle.

ACKNOWLEDGEMENTS

This work took place in the framework of the OpenLab 'Electronics and Systems for Automotive' combining IMS laboratory and PSA Groupe company.

REFERENCES

A. Chebly, G. Tagne, R.T. and Charara, A. (2015). Local trajectory planning and tracking for autonomous vehicle navigation using clothoid tentacles method. *In proceedings of International IEEE Conference on Intelligent Vehicles Symposium (IV)*.

Andrew-Fields, R. (2014). *Continuous Control Artificial Potential Function Methods and Optimal Control*. Ph.D. thesis, Air Force Institute of Technology.

Ge, S. and Cui, Y. (2002). Dynamic motion planning for mobile robots using potential field method. *Autonomous Robots*, 13, 207–222.

Inarn, C., Melchior, P., Metoui, B., and Oustaloup, A. (2012). Robust path planning for 3D dynamic environment based on fractional attractive force. *5th IFAC Symposium on Fractional Differentiation and Its Applications (IFAC FDA'12)*.

Liu, Y., Zhang, X., Guan, X., and Delahayel, D. (2016). Potential odor intensity grid based UAV path planning algorithm with particle swarm optimization approach. *Mathematical Problems in Engineering*, 2016, 1–16.

Makarem, L. and Gillet, D. (2011). Decentralized coordination of autonomous vehicles. *In proceedings of the 18th IFAC World Congress*, 44, 13046–13051.

Melchior, P., Orsoni, B., Lavialle, O., Poty, A., and Oustaloup, A. (2003). Consideration of obstacle danger level in path planning using A^* and fast-marching optimisation: comparative study. *Signal processing*, 83, 2387–2396.

Melchior, P., Orsoni, B., and Oustaloup, A. (2001). Weyl fractional potential in path planning. *Proceedings of the Sixth IEEE ECC'2001*.

Metoui, B., Melchior, P., Najar, S., Abdelkrim, M., and Oustaloup, A. (2009). Robust path planning for dynamic environment based on fractional attractive force. *Sixth IEEE International Multi-Conference on Systems, Signals and Devices (IEEE SSD'09)*.

Morand, A., Moreau, X., Melchior, P., Moze, M., and Guillemard, F. (2016). Crone cruise control system. *IEEE Transactions on Vehicular Technology*, 65, 15–28.

Oustaloup, A., Sabatier, J., Lanusse, P., and Melchior, P. (2014). *Fractional Order Differentiation and Robust Control Design: CRONE, H-infinity and Motion Control*. Wiley-ISTE, Paris.

Shibata, N., Sugiyama, S., and Wada, T. (2014). Collision avoidance control with steering using velocity potential field. *IEEE Intelligent Vehicles Symposium*.

Zhan, W., Wang, W., Chen, N., and Wang, C. (2014). Efficient UAV path planning with multiconstraints in a 3D battlefield environnement. *Mathematical Problems in Engineering*, 2014, 1–12.